

Compare Results

Old File:

acp-2022-339-manuscript-version1.pdf

16 pages (688 KB)

5/13/2022 10:46:03 AM

versus

New File:

**Differences in Droplet Growth Model of
Functionalized Insoluble Aerosol Surfaces-
ACP_edition_3.pdf**

12 pages (697 KB)

8/20/2022 10:17:30 AM

Total Changes

251

Text only comparison

Content

51 Replacements
92 Insertions
108 Deletions

Styling and Annotations

0 Styling
0 Annotations

[Go to First Change \(page 1\)](#)

A Single Parameter Hygroscopicity Model for Functionalized Insoluble Aerosol Surfaces

Chun-Ning Mao¹, Kanishk Gohil¹, Akua Asa-Awuku^{1,2}

¹ Department of Chemical and Biomolecular Engineering, University of Maryland, College Park, MD 20742 USA

5 ² Department of Chemistry and Biochemistry, University of Maryland, College Park, MD 20742 USA

Correspondence to: Akua A. Asa-Awuku (asaawuku@umd.edu)

Abstract. The impact of molecular level surface chemistry for aerosol water-uptake and droplet growth is not well understood. In this work, spherical, non-porous, monodisperse Polystyrene Latex (PSL) particles treated with different surface functional groups are exploited to isolate the effects of aerosol surface chemistry for droplet activation. PSL is effectively water-insoluble and changes in the particle surface may be considered a critical factor in the initial water-uptake of water insoluble material. The droplet growth of two surface modified types of PSL (PSL-NH₂ and PSL-COOH) along with plain PSL was measured in a supersaturated environment with a Cloud Condensation Nuclei Counter (CCNC). Three droplet growth models - traditional Köhler (TK), Flory-Huggins Köhler (FHK) and the Frenkel-Halsey-Hill adsorption theory (FHH-AT) were compared to experimental data. The experimentally determined single hygroscopicity parameter, κ , was found in the range from 0.002 to 0.04. The traditional Köhler prediction assumes Raoult's law solute dissolution and underestimates the water-uptake ability of the PSL particles. FHK can be applied to polymeric aerosol; however, FHK assumes the polymer is soluble and hydrophilic. Thus, the FHK model generates a negative result for hydrophobic PSL and predicts non-activation behavior that disagrees with the experimental observation. The FHH-AT model assumes that a particle is water-insoluble and can be fit with 2 empirical parameters (A_{FHH} and B_{FHH}). The FHH-AT prediction agrees with the experimental data and can differentiate the water uptake behavior of the particles due to surface modification of PSL surface. PSL-NH₂ exhibits slightly higher hygroscopicity than the PSL-COOH, while plain PSL is the least hygroscopic among the three. This result is consistent with the polarity of surface functional groups and their affinity to water molecules. Thus, changes in A_{FHH} and B_{FHH} can be quantified when surface modification is isolated for the study of water-uptake. The fitted A_{FHH} for PSL-NH₂, PSL-COOH and plain PSL is 0.23, 0.21 and 0.18 when B_{FHH} is unity. To simplify the use of FHH-AT for use in cloud activation models, we also present and test a new single parameter framework for insoluble compounds, κ_{FHH} . κ_{FHH} is within 5% agreement of the experimental data and can be applied to describe a single-parameter hygroscopicity for water-insoluble aerosol with surface modified properties.

1. Introduction.

Heterogeneous water-vapor condensation occurs for both soluble (Rose et al., 2008) and insoluble (Dalirian et al., 2018; Koehler et al., 2009; Kumar et al., 2009) particles. Traditionally, the cloud condensation nuclei (CCN) activation behavior is described by Köhler theory (Köhler, 1936). In traditional Köhler (TK) theory, the droplet is assumed to be dilute, and the water activity follows Raoult's law; such that the water activity equals the water mole fraction, and the dilute droplet water activity coefficient is assumed to be unity. For water-soluble particles like inorganic ammonium sulfate (Rose et al., 2008) and sucrose (Dawson et al., 2020; Gohil and Asa-Awuku, 2022), TK can predict their water uptake behavior. However, TK does not work so well for atmospherically relevant and abundant particles that are partially water soluble or water insoluble, less than a concentration of 5×10^{-4} (Kumar et al., 2009; Petters and Kreidenweis, 2008; Tang et al., 2016). Thus, alternative droplet growth models for the partial and insoluble particles are needed.

Flory Huggins Köhler (FHK)(Petters et al., 2009) is one example of a droplet growth model specifically applied to the water soluble polymers. FHK has been shown to work well for long-chained polymers such as gelatin, polyethylene glycol and polylactic acid (Mao et al., 2021; Petters et al., 2006, 2009). It uses a one fitting parameter that describes solvation and most recently was incorporated into a single-parameter hygroscopicity term that describes the water-uptake of water-soluble aerosol (Mao et al., 2021).

The droplet formation of water-insoluble particles has been previously described with adsorption activation models (Hatch et al., 2012; Kumar et al., 2009; Lintis et al., 2021; Malek et al., 2022; Navea et al., 2017; Pajunoja et al., 2015; Tang et al., 2016). Brunauer, Emmett, and Teller adsorption isotherm models are typically applied for multilayer adsorption analysis of water uptake

on clays (Hatch et al., 2012) and fly ash (Navea et al., 2017). Lintis et al., 2021 applied the Dubinin-Serpinsky model for soot and concluded that nucleation occurred at oxidized and hydrophilic surface sites on the soot. Pajunoja et al. measured the TK hygroscopicity for SOA and demonstrated that the droplet growth of organic compounds with low O:C ratio was an adsorption-dominated process for both sub – and super-saturated water vapor conditions. Kumar et al. 2009 showed that the droplet activation of mineral dust could be described well using the Frenkel-Halsey-Hill adsorption theory (FHH-AT).

FHH-AT determines droplet growth with the help of 2 empirical parameters defined as A_{FHH} and B_{FHH} (Sorjamaa and Laaksonen, 2007a). The parameter A_{FHH} is related to the interaction of the first layer of water and the particle surface, while the B_{FHH} represents the interaction between other layers of water molecules and the particles. Furthermore, it is postulated that A_{FHH} should range from 0.1 to 3.0, and B_{FHH} should be within range of 0.5 to 3.0 for mineral dust aerosols (Kumar et al., 2009). However, the reported and applied A_{FHH} and B_{FHH} parameters have varied significantly in literature. For example, Karydis et al. 2017 used the FHH-AT model to simulate the aerosol indirect effect of insoluble mineral dust CCN with an A_{FHH} and B_{FHH} of 2.25 ± 0.75 , and 1.20 ± 0.10 respectively. Furthermore, Karydis et al., 2017 concluded that the global CCN number would decrease 10% for mineral dust with the use of those values. Hatch et al., 2014 measured montmorillonite dust and found that the A_{FHH} and B_{FHH} was 98 ± 22 and 1.79 ± 0.11 and the A_{FHH} and B_{FHH} was 75 ± 17 and 1.77 ± 0.11 for illite, respectively. Particles of intermediate polarity and high porosity may lead to a higher CCN activity (Koehler et al., 2009) and Hatch et al., 2012 attributed the high value of A_{FHH} to the surface chemistry and the porosity of the clays.

Specifically, porosity leads to a higher perceived hygroscopicity because water molecules fill the microporous structure. Thus, it should be noted that in the aforementioned studies, the porosity of insoluble particles complicates the study of aerosol water-uptake and influences the role of aerosol chemistry that impacts the CCN activity. Moreover, the use of two parameters adds an additional degree of freedom that makes the direct comparison of different chemical species challenging; there may be multiple pairs A_{FHH} and B_{FHH} solutions for a single compound with or without porous structure. As a result, direct experimental measurement of the hygroscopicity of non-porous and spherical nuclei is important to understand the adsorption water uptake ability of atmospheric aerosol.

To better understand the activation behavior of insoluble particles, we study the CCN activity of spherical, non-porous polystyrene latex (PSL) particles using the Cloud Condensational Nuclei Counter (CCNC) (Roberts and Nenes, 2005). PSL is a common material used for instrumentation calibration and model examination for aerosol optical properties. (Miles et al., 2011; Pettersson et al., 2004; Singh et al., 2014). They are spherical, uniform in size, and do not dissolve in water. The surfaces of PSL particles are hydrophobic, but can be manufactured to have a high density of hydrophilic sites (Ottewill and Vincent, 1972). Different functional groups like carboxyl (-COOH) or amine (-NH₂) groups can be added to the PSL surface to create hydrophilic adsorption sites. Previous studies have shown that surface chemistry of the insoluble particles affect ice nucleation (Cziczo et al., 2009; Koehler et al., 2009; Reitz et al., 2011; Sullivan et al., 2010). But little is known about the influence of surface chemistry for liquid cloud droplet activation.

To our knowledge, few studies have explored the effects of molecular level particle surface changes for CCN and droplet formation. Mainly, water-soluble aerosol that contribute solute to the solution and modify droplet properties has been of great interest. Any changes at the surface of soluble aerosol are often overshadowed by the effects of solute dissolution if the solute is water-soluble. Additionally, to understand impacts of functionalized surfaces, the surface area or particle size of an aerosol must be well known. Given these constraints, spherical PSL aerosol with and without a functionalized surface provides an opportunity to advance the contributions of molecular surfaces to the discussion of water-uptake.

In the following sections, we examine the impact of surface chemistry to the CCN activity in both the Traditional Köhler (TK), Flory Huggins Köhler (FHK) and the FHH-AT model. The first two models are generally applied to water-soluble compounds while the FHH-AT is for water-insoluble particles. Furthermore, FHK is specifically designed for high-molecular weight polymers like PSL and therefore briefly considered. The following work also compares measurements to three hygroscopicity prediction models. Two single parameter hygroscopicity representations have been previously derived using TK (Petters and Kreidenweis, 2007) and FHK (Mao et al., 2021) assumptions. Additionally, we derive a third theoretical hygroscopicity parameter using the FHH-AT model and analyze the role of surface chemistry in the adsorption based hygroscopicity. Thus, the following data and analysis provides insight into the water-uptake of water-insoluble particles and the impact of surface modified functional groups for the perceived aerosol hygroscopicity and droplet formation.

2. Experimental Procedure.

2.1 Polystyrene Latex (PSL) Composition and Size

95 Four different particle sizes, ~100nm, 200nm, 300nm and 500nm and three different PSL particles (plain, surface modified with amine functional group, -NH₂, and carboxyl functional group, -COOH) were purchased (Lab 261®). The sizes provided by the manufacturer are determined with dynamic light scattering (DLS) techniques. In this study, we verify the size and report the electrical mobility measured particle size (D_d) of the PSL particles with a Differential Mobility Analyzer, DMA (TSI 3080) and Condensation Particle Sizer (TSI 3776) operated in size scanning mode (Wang and Flagan, 1990). The measured geometric mean size was within ~10% difference of the manufacturer's reported particle sizes (Table 1).

2.2 Aerosol Generation

105 0.4 ml of the PSL particle solution was diluted in 50ml ultra-purified water (Millipore®, with conductivity < 18.8MΩ). Wet particles were then generated with a constant output atomizer (TSI, 3076). Wet droplets were then passed through two silica gel dryers and the relative humidity was 5% after passing through the dryers. After drying, large particles were removed by a 0.71 cm impactor to prevent the multiple charging errors. Poly-disperse particles are charged and sampled by an electrostatic size classifier, specifically a Differential Mobility Analyzer (TSI, DMA 3080). The DMA was set to select the size of the PSL particles. The PSL particles are then passed through a Condensation Particle Counter (CPC, TSI 3776) with a flow rate of 0.3 L min⁻¹ and a CCNC. The particle density counted by the CPC is the condensation number concentration (CN) and is measured at rate of 1 Hz. The sheath and sample flow ratio are 10:1 in both the CPC and CCNC.

2.3 The Critical Supersaturation of PSL

115 The CCN activity for the selected particle size was measured with a continuous flow stream-wise thermal gradient Cloud Condensation Nuclei Counter (DMT CCN100) (Roberts and Nenes, 2005). A brief introduction is provided here and readers are directed to the (Roberts and Nenes, 2005) for a more detailed discussion of the instrument. The CCNC is a column with a wet inner surface. Three thermal electrical controllers modify temperatures on the top, in the middle, and at the bottom of the CCNC column to establish a constant temperature gradient. A supersaturation is generated at the center of the column as air moves from the top to the bottom (Hoppel et al., 1979). The sampled particles in the CCNC column provide surface for the occurrence of the heterogeneous condensation. An optical particle counter (OPC) at the bottom of the column, counts the particles that form droplets greater than 0.75 μm and provides the cloud condensation number concentration (CCN) every 1 Hz. Instrument supersaturations were achieved by modifying both inlet flowrate and the temperature gradient in the CCNC. Each supersaturation was calibrated using ammonium sulfate and Scanning Mobility CCN Analysis (SMCA) (Moore et al., 2010).

120 CCN activity is the ratio of number droplets to total aerosol (CCN/CN) measured at a given supersaturation and constant particle size (D_d). For each supersaturation, temperatures and flows are held constant for 10 minutes and CCN and CN data are measured every second. The CCN and CN concentration is then averaged in the 8th minute. The CCN activation for each sample is reported from 0.1 to 1.4% supersaturation. Critical supersaturation (s_c) for a given particle size (D_d) is defined at 50% efficiency growth of the CCN (i.e., CCN/CN=0.5). A smaller s_c for a constant D_d indicates that the particles are more hygroscopic. The s_c for all twelve PSL are listed in Table 1. The activation curves for all twelve PSL samples are provided in Supplemental Materials (Figure S-1). The measured s_c and D_d values are used to compute and compare subsequent particle CCN activation and hygroscopicity.

130

3. Theory and Analysis

The saturation ratio at the droplet surface can be generally described as follows.

$$S = a_w \exp\left(\frac{A}{D}\right) ; \text{ and } A = \frac{4M_w\sigma_w}{RT\rho_w} \quad (1)$$

135 where S is the saturation ratio; a_w is the water activity of the solution and D is the wet diameter of the droplet. The exponential term is known as the Kelvin term and describes the homogeneous nucleation of the droplet solvent. Thus, A is generally constant and is a function of the universal gas constant (R), the pure water droplet surface tension (σ_w), temperature (T), density (ρ_w) and molecular weight (M_w). Heterogeneous nucleation is considered in the water activity term. As aforementioned, for water-soluble

inorganic salts and organics, (e.g., ammonium sulfate and sucrose) the water activity is approximated with Raoult's law and the water mole fraction, x_w .

140 Petters and Kreidenweis, 2007 employed Raoult's law to develop a single hygroscopicity parameter representation, κ , as follows,

$$\frac{1}{a_w} = 1 + \kappa \frac{v_s}{v_w}, \quad (2)$$

145 Where v_s is the total volume of the dry particle and v_w is the total volume of the water in a droplet. The κ in (2) is defined as the intrinsic hygroscopicity parameter of the compound, denoted by κ_{int} . If one assumes a dilute droplet, such that $a_w = 1$, κ_{int} can be solved from known solute and solvent properties such that $\kappa_{int} = v \frac{M_w \rho_s}{M_s \rho_w}$ (Sullivan et al., 2009). Where M_w is the molecular weight of water; M_s is the molecular weight of the dry particle; ρ_w is the density of water; ρ_s is the density of the dry particle; v is the van't Hoff coefficient and is assumed to be one. If PSL is a polymer with $\sim 100,000$ g mol⁻¹ molecular weight and a density of 1.06 g cm⁻³, $\kappa_{int} \sim 0.0002$, is a small number and approaches zero. One can also derive a hygroscopicity parameter based on TK, κ_{TK} , directly from measured experimental s_c and D_d data (Petters and Kreidenweis, 2007)

$$150 \quad \kappa_{TK} = \frac{4A^3}{27D_d^3 \ln^2 s_c} \quad (3)$$

$\kappa_{int} = \kappa_{TK} = 0.604$ for ammonium sulfate (Rose et al., 2008). The intrinsic and experimentally derived values also agree well for water-soluble compounds and partially soluble organics (Dawson et al., 2020; Peng et al., 2021, 2022).

Traditional Köhler theory calculations from theory and measurement tend to disagree for high molecular weight organics, such as polymers (Petters et al., 2006, 2009). To calculate the water activity of high molecular weight compounds, Petters et al., 155 2006, 2009 combined the water activity of Flory-Huggins (Flory, 1942) with the Köhler theory for polymeric aerosols. Mao et al., 2021 derived a single parameter based hygroscopicity representation, κ_{FHK} as follows,

$$\kappa_{FHK} = \frac{1-\varphi}{\varphi} \left[-1 + \frac{1}{(1-\varphi) \exp[(1-F)\varphi + \chi\varphi^2]} \right], \quad (4)$$

160 where φ is the volume fraction of the polymer. F is the reciprocal of the chain segments of the polymer equal to the ratio of the molecular volume of water and the solute and χ is the Flory-Huggins interaction parameter. Measured particle diameter, D_d , and s_c data are used to define empirical fits of χ and subsequently determine, κ_{FHK} .

Insoluble aerosol droplet activation is best described by an adsorption thermodynamic droplet growth model (Kumar et al., 2009). Sorjamaa and Laaksonen, 2007a suggested the Frenkel-Halsey-Hill adsorption theory (FHH-AT) to define the a_w using the isotherm as follows,

$$a_w = \exp(-A_{FHH} \theta^{-B_{FHH}}) \quad \text{and} \quad \theta = \frac{D - D_d}{2D_w}, \quad (5)$$

165 where θ is the surface coverage, and describes the layers of water molecules adsorbed on to the dry particle surface (Sorjamaa and Laaksonen, 2007b). D_w is the diameter of a single water molecule and equals to 0.275 nm. A_{FHH} and B_{FHH} are compound specific empirical parameters. The FHH-AT parameters can be estimated by fitting the FHH-AT with s_c and D_d CCN measurement data (Herich et al., 2009; Kumar et al., 2009).

170 To date, a single parameter hygroscopicity representation based on adsorption droplet growth does not exist in the current literature. In this work, we derive an experimental and theoretical adsorption hygroscopicity, $\kappa_{FHH,exp}$ and $\kappa_{FHH,the}$ respectively. If the critical wet droplet diameter, $D_{p,c}$, is known, $\kappa_{FHH,exp}$, can then be expressed as a function of D_d and $D_{p,c}$ as follows

$$\kappa_{FHH,exp} = f(D_d, D_{p,c}) = \frac{6\theta D_w}{D_d} \left(\frac{1}{\exp(-A_{FHH} \theta^{-B_{FHH}})} - 1 \right), \quad (6)$$

Theoretically, droplet activation occurs when the derivative of the Köhler curve equals to zero ($\frac{ds}{dD_{p,c}} = 0$). Hence the relation between critical surface coverage and the dry particle size is constrained with the following equation,

$$1 - \frac{2\theta_c D_w}{D_d} = \left(\frac{2AD_w}{A_{FHH} B_{FHH} D_d^2} \right)^{1/2} \theta_c^{\frac{B_{FHH}+1}{2}}, \quad (7)$$

The critical surface coverage, θ_c , is defined at the point where droplet activation occurs, and is obtained by solving Eq. (7). As a result, the theoretical hygroscopicity of FHH-AT is derived,

$$\kappa_{FHH,the} = f(D_d) = \frac{6D_w}{D_d} A_{FHH} \theta_c^{-B_{FHH}+1}, \quad (8)$$

Readers should refer to Appendix A for additional derivation details.

180

4. Results and Discussion

4.1 The CCN activity for different types of PSL.

Table 1 shows the mobility diameter of PSL and their corresponding critical supersaturation. Particle size matters most for water-uptake and thus larger particles (~500nm) exposed to a constant supersaturation activate earlier than smaller aerosol (~100nm) (Dusek et al., 2006). For example, PSL-NH₂ particles with 85 nm diameters activate at 1.42% supersaturation while particles with 375nm activate at 0.33% supersaturation. PSL-COOH and the plain PSL show a similar trend as well. The data suggests that PSL particles are wettable and hygroscopic, more so than particles with $\kappa = 0$. The parameters in Table 1 are used to predict CCN activation (s_c - D_d pairs) in Figure 1(a) and (b). The red dashed line in Figure 1 shows the traditional Köhler prediction for ammonium sulfate ($\kappa_{int} = 0.604$) for comparison purposes. All PSL particles are much less hygroscopic than ammonium sulfate ($\kappa_{int} = 0.604$) with larger hygroscopicity than theoretical values derived from known solute properties ($\kappa_{int} = 0.0002$). Traditional Köhler theory significantly underpredicts particle activation and droplet growth of PSL particles.

Table 1 also shows the fitted parameters for the FHK, and FHH-AT models required to subsequently calculate κ_{FHK} and $\kappa_{FHH,the}$. Both FHK and FHH-AT models have additional degrees of freedom compared to the traditional Köhler theory. In the FHK model, the molar volume becomes negligible and the water-polymer interaction parameter (χ), drives the droplet activation. χ describes the repulsive and attractive force between the solvent and the polymer. A χ smaller than 0.5 is an indication of miscibility and that water is a “good solvent” (Pethrick, 2004). χ is the only empirical free parameter in this study and when fitted to all three types of PSL, $\chi > 0.5$ and confirms the assumption that PSL particles are water insoluble. In Figure 1a, the FHK model with only one free fitting parameter more closely agrees with experimental data than the TK theory (red solid lines).

Two empirical parameters (A_{FHH} and B_{FHH}) for the FHH-AT model are reported for each type of the PSL. The FHH-AT model with two degrees of freedom agrees with the experimental data better than the traditional Köhler theory model (Figure 1b). However, multiple solutions of A_{FHH} and B_{FHH} may exist. The fit results for plain type PSL estimate $A_{FHH} = 0.17$ and $B_{FHH} = 0.99$; A_{FHH} is 0.3 and B_{FHH} is 1.08 for carboxyl functional group modified PSL; A_{FHH} is 0.11 and B_{FHH} is 0.83 for amine functional group modified PSL. Differences in the A_{FHH} and B_{FHH} values confirm that the FHH-AT model is sensitive to molecular level chemistry and can distinguish changes in surface chemistry. PSL-COOH shows a higher attraction to water molecules than the plain PSL. However, PSL-NH₂ is the most hygroscopic among the three types of the PSL and the $A_{FHH} = 0.11$ and the $B_{FHH} = 0.83$ of PSL-NH₂ are the lowest values among all three types. If A_{FHH} represents the interaction between the first layer water molecules and the surface of the PSL particles, a higher A_{FHH} value implies higher attractive forces. Thus, the unconstrained FHH-AT parameter solutions must be reassessed.

The only chemical difference between the three types of PSL is due to surface modification. The attraction force between the particle core and the layers of the water molecules should be the same. Thus, a second constrained best-fit solution exists if we restrict $B_{FHH} = 1$ (Table 1). The constrained and fitted A_{FHH} is 0.18 for plain PSL, 0.21 for PSL-COOH and 0.23 for PSL-NH₂ (Table 1, Figure 1b). With the constrained solution, the higher A_{FHH} is consistent with the most hygroscopic aerosol species. In Figure 1b, the FHH-AT model prediction agrees well with the experimentally measured s_c - D_d data more than traditional Köhler Theory. This agreement with data is true for both the best-fit constrained ($B_{FHH} = 1$, Figure 1b) and unconstrained A_{FHH} and B_{FHH} values (not shown).

Table 1. Important aerosol physical properties and parameters used to derive droplet growth.

κ_{int} (-)	χ (-)	A_{FHH} (-)	B_{FHH} (-)	Surface Modification	D_d (nm)	s_c (%)
0.0002	0.56	0.18	1	Plain	85	1.27
					250	0.43
					310	0.42
					474	0.33
0.0002	0.54	0.21	1	-COOH Carboxyl	89	1.08
					223	0.61
					331	0.36
0.0002	0.57	0.23	1	-NH ₂ Amine	472	0.25
					85	1.42
					195	0.63
					278	0.35
					375	0.33

4.2 The Impact of Surface Chemistry to Hygroscopicity of PSL

The perceived single parameter hygroscopicity, κ_{TK} and the κ_{FHH} can be derived from traditional Köhler and FHH-AT models, respectively (Figure 2). In TK, the theoretical hygroscopicity is a constant value independent to the size of the particles. In Figure 2 (a), the red solid horizontal line shows $\kappa_{int} = 0.0002$. The red open symbols (circle, square and triangle) are the hygroscopicity from measured data (Equation 3) of the respective PSL particles. The experimental κ_{TK} values from traditional Köhler theory range from 0.002 to 0.04. Additionally, κ_{TK} of the PSL are size dependant and are larger than κ_{int} . Thus, TK should not be applied to predict the droplet growth and single parameter hygroscopicity of insoluble PSL particles.

In addition, FHK should not be used to predict droplet growth of PSL. Although the FHK model agrees well with s_c - D_d data (Figure 1a), the derived hygroscopicity is problematic and nonsensical (therefore not shown). FHK assumes that the hydrophilic polymer swells in the water droplet and the interaction parameter represents the molecular force between water and polymer. χ values larger than 0.5 derived from PSL-NH₂, PSL-COOH and plain PSL subsequently estimate negative and implausible κ_{FHK} values. The experimental data indicate that the PSL indeed grow into droplets and have a positive hygroscopicity. Thus, FHK should not be applied to water-insoluble polymers like PSL.

The hygroscopicity values derived from the FHH-AT model are plausible and show the best agreement between theory and experiment (Figure 2). Both theoretical ($\kappa_{FHH,the}$) and experimental ($\kappa_{FHH,exp}$) hygroscopicity values from FHH-AT model are less than the κ_{TK} (red open symbols), but higher than a constant κ_{int} value of 0.0002. $\kappa_{FHH,exp}$ and $\kappa_{FHH,the}$ for all twelve PSL are within 5% of each other. The small deviation between $\kappa_{FHH,the}$ and $\kappa_{FHH,exp}$ demonstrate that the adsorption model is best for PSL. For insoluble particles, the experimental single parameter hygroscopicity is size dependent and decreases with an increasing diameter (Figure 2). This is because the core does not dissolve, and the total volume of the dry particle (Equation 2) does not fully participate in the water uptake. The particle surface of an insoluble particle is proportional to the square of the size and dominates the adsorption-based water activation behavior. However, the single parameter hygroscopicity is defined by the volume ratio of the solute and the solvent, which is proportional to the cube of the size. In adsorption driven growth, the core inactive particle volume enlarges when the particle size increases and as a result the perceived size dependence in the experimental hygroscopicity is exhibited. The FHH-AT model accounts for the core volume contribution to the water activation in the B_{FHH} parameter. In the special case of PSL particles, B_{FHH} happens to be 1 (Table 1), hence the $\kappa_{FHH,the}$ is directly the reciprocal of the dry size (Equation

8). $\kappa_{FHH,the}$ accurately describes the inactive core volume behavior, demonstrating a decrease of hygroscopicity with an increasing particle size. Larger particles still activate earlier than smaller particles. For example, 500nm particles activate earlier than 100 nm particles at 0.3% supersaturation due to a larger surface area which provides more active sites for adsorption. Moreover, FHH-AT hygroscopicity is also sensitive to the small differences in surface chemistry. The theoretical prediction for the CCN activation of PSL-NH₂ particles (the dashed line) is larger than PSL-COOH (dashed-dotted line), while the plain PSL is the lowest (solid line).

245

250 5. Summary and Implications

PSL are spherical, insoluble, non-porous, mono-dispersed particles and their surface can be modified to be hydrophilic or hydrophobic. The performance of the adsorption model is better than the traditional Köhler for PSL particles; experimentally derived κ_{TK} predicts a higher hygroscopicity and κ_{int} approaches zero. κ_{FHK} is negative for the insoluble particles and is inconsistent with the growing droplets. The single parameter hygroscopicity of the FHH-AT model replicates the small differences of the functionalized surface. $\kappa_{FHH,exp}$ and $\kappa_{FHH,the}$ are only within 5% differences. $\kappa_{FHH,the}$ decreases with an increasing particle size, demonstrating the inactivity of the inner core of larger particles.

255

Using a droplet growth model with additional degrees of freedom improves the droplet growth prediction of PSL. The FHH-AT model is typically applied to effectively water-insoluble particles and the adsorption model agrees well with the experimental droplet growth data for hydrophobic and hydrophilic functionalized surfaces. This finding is consistent with the current body of work that highlights the bulk aerosol composition as a critical factor in aerosol water uptake. However, the addition of polar functional groups to the surface of the water-insoluble particle exhibits discernible differences in activation and suggests that for atmospheric insoluble aerosol (e.g., soot, mineral dust) the modified surface chemistry should not be ignored.

260

We found from experiments that B_{FHH} was ≈ 1 for pure and coated PSL particles. This implied that for the samples studied in this work, B_{FHH} could be constrained to 1 to determine the A_{FHH} and postulate the contribution of surface chemistry on the CCN activation. The method of constraining B_{FHH} can distinguish both the surface modification and potential coatings when the B_{FHH} of the core is known. If B_{FHH} of the pure core is known, only A_{FHH} needs to be measured and accounted for to estimate water uptake ability. Furthermore, it was found that if both A_{FHH} and B_{FHH} are left unconstrained, the values of A_{FHH} come out to be within 5% of the A_{FHH} when B_{FHH} is constrained. It is also important to note from Eq. (A10) that the κ_{FHH} depends only on the surface properties of the compound (A_{FHH}) when B_{FHH} is constrained to unity. This can imply that the hygroscopic properties of the compound will only depend on the hydrophilic or hydrophobic properties of the functionalized surface regardless of the bulk properties if B_{FHH} is constrained to unity. In other words, extensions of this work could potentially apply A_{FHH} water-adsorption properties to similarly functionalized surfaces with different particle core compositions (i.e., varying B_{FHH}).

265

270

The findings presented here may be extended to atmospherically relevant insoluble particles that may be either coated or surface oxidized during different chemical processes. In ambient measurement, quite rarely is the composition of the surface and core simultaneously known; single particle measurements are required to discern the individual composition and morphology. Thus, the singular κ_{FHH} value provides an important utility. Regardless of whether the FHH-AT model is constrained, κ_{FHH} reduces the the degrees of freedom of the model and can discern changes in surface chemistry. It should be noted that the extent to which the adsorption-driven droplet growth can be applied to increasingly hydrophilic aerosol is uncertain but has been explored. Readers who are interested in the adsorption driven water uptake ability of partially soluble compounds are referred to a companion paper Gohil et al, *submitted*. In summary, water-insoluble aerosol can adsorb water and if their surfaces have been oxidized or functionalized with polar groups the aerosol can enhance their efficiency for water-uptake.

275

280

Appendix

A typical droplet growth model is expressed as,

285

$$S = a_w \cdot \exp\left(\frac{A}{D_p}\right), \quad (\text{A.1})$$

where S is saturation, a_w is the water activity of the solution and D_p is the diameter of the droplet. A is a coefficient related to pure water droplet properties which is given as,

$$A = \frac{4M_w\sigma_w}{RT\rho_w} \quad (\text{A.2})$$

290 Where M_w is the molecular weight of water, R is the gas constant, T is the temperature and ρ_w is the density of water. σ_w is the surface tension of the droplet and is assumed to be the same as that of pure water.

If the solute is effectively insoluble, then the water activity term is expressed using the FHH-AT isotherm as,

$$a_w = \exp(-A_{FHH}\theta^{-B_{FHH}}), \quad (\text{A.3})$$

where θ is the surface coverage term and is related to a_w with the help of compound-specific empirical parameters (A_{FHH} , B_{FHH}). A simplified representation of θ is given as,

$$295 \quad \theta = \frac{D_p - D_d}{2D_w}, \quad (\text{A.4})$$

where D_p is the droplet size, D_d is the dry particle size, and D_w is the diameter of one water molecule. (A.3) can be equated with the a_w parameterization defined in terms of the single hygroscopicity parameter (κ) which is expressed as,

$$a_w = \exp(-A_{FHH} \cdot \theta^{-B_{FHH}}) = \left[1 + \kappa \cdot \frac{v_s}{v_w}\right]^{-1}, \quad (\text{A.5})$$

Rearranging (A.5) provides the expression for κ_{FHH} as,

$$300 \quad \kappa_{FHH} = \frac{6\theta D_w}{\exp(-A_{FHH}\theta^{-B_{FHH}}) - 1}, \quad (\text{A.6})$$

(A.6) is the function of the measured D_d and D_p derived corresponding the point of activation. (A.6) can be further simplified by making physically relevant mathematical assumptions for (A.5). The right-hand side of (A.5) can be simplified using the Taylor series expansion for an exponential function such that,

$$\exp(-A_{FHH}\theta^{-B_{FHH}}) = 1 + (-A_{FHH}\theta^{-B_{FHH}}) + (-A_{FHH}\theta^{-B_{FHH}})^2 + (-A_{FHH}\theta^{-B_{FHH}})^3 + \dots, \quad (\text{A.7})$$

305 Since $-A_{FHH}\theta^{-B_{FHH}} \ll 1$, (A.7) can be restated as,

$$\exp(-A_{FHH}\theta^{-B_{FHH}}) \approx 1 + (-A_{FHH}\theta^{-B_{FHH}}), \quad (\text{A.8})$$

The left-hand side of (A.5) can be simplified under the assumption that $v_w \gg v_s$ such that,

$$\left[1 + \kappa \cdot \frac{v_s}{v_w}\right]^{-1} \approx 1 - \kappa \cdot \frac{v_s}{v_w}, \quad (\text{A.9})$$

Combining (A.8) and (A.9) provides a reduced theoretical expression for κ_{FHH} ,

$$310 \quad \kappa_{FHH,th} = \frac{6D_w}{D_d} A_{FHH} \theta^{-B_{FHH}+1}, \quad (\text{A.10})$$

(A.10) contains θ defined as the point of activation such that $\theta = \theta_c$. θ_c is determined by taking the first derivative of (A.1) and equating it to 0 to represent the point of activation such that,


$$\frac{dS}{dD_p} = \frac{d}{dD_p} \left(-A_{FHH} \cdot \left[\frac{D_p - D_d}{2 \cdot D_w} \right]^{-B_{FHH}} \cdot \exp\left(\frac{A}{D}\right) \right) = 0, \quad (\text{A.11})$$

$$1 - \frac{2\theta_c D_w}{D_d} = \left(\frac{2AD_w}{A_{FHH} B_{FHH} D_d^2} \right) \theta_c^{\frac{3B_{FHH}+1}{2}}, \quad (\text{A.12})$$

315 References


Cziczko, D. J., Froyd, K. D., Gallavardin, S. J., Moehler, O., Benz, S., Saathoff, H. and Murphy, D. M.: Deactivation of ice nuclei due to atmospherically relevant surface coatings, *Environ. Res. Lett.*, 4(4), 044013, doi:10.1088/1748-9326/4/4/044013, 2009.

320

 Dalirian, M., Ylisirniö, A., Buchholz, A., Schlesinger, D., Ström, J., Virtanen, A. and Riipinen, I.: Cloud droplet activation of black carbon particles coated with organic compounds of varying solubility, *Atmos. Chem. Phys.*, 18(16), 12477–12489, doi:10.5194/ACP-18-12477-2018, 2018.


Dawson, J. N., Malek, K. A., Razafindrambina, P. N., Raymond, T. M., Dutcher, D. D., Asa-Awuku, A. A. and Freedman, M. A.: Direct Comparison of the Submicron Aerosol Hygroscopicity of Water-Soluble Sugars, *ACS Earth Sp. Chem.*, 4(12), 2215–2226, doi:10.1021/ACSEARTHSPACECHEM.0C00159/SUPPL_FILE/SP0C00159_SI_001.PDF, 2020.

325

 Dusek, U., Frank, G. P., Hildebrandt, L., Curtius, J., Schneider, J., Walter, S., Chand, D., Drewnick, F., Hings, S., Jung, D., Borrmann, S. and Andreae, M. O.: Size matters more than chemistry for cloud-nucleating ability of aerosol particles, *Science* (80-.), 312(5778), 1375–1378, doi:10.1126/SCIENCE.1125261/SUPPL_FILE/DUSEK.SOM.PDF, 2006.


Flory, P. J.: The Thermodynamics of High Polymer Solutions. V. Phase Equilibria in the Ternary System: Polymer 1-Polymer 2-Solvent The, *Stat. Mech. Cross-Linked Polym. Networks II. Swelling J. Chem. Phys.*, 10, 279, doi:10.1063/1.1723621, 1942.


330

 Gohil, K. and Asa-Awuku, A. A.: Cloud condensation nuclei (CCN) activity analysis of low-hygroscopicity aerosols using the aerodynamic aerosol classifier (AAC), *Atmos. Meas. Tech.*, 15(4), 1007–1019, doi:10.5194/AMT-15-1007-2022, 2022.

Hatch, C. D., Wiese, J. S., Crane, C. C., Harris, K. J., Kloss, H. G. and Baltrusaitis, J.: Water Adsorption on Clay Minerals As a Function of Relative Humidity: Application of BET and Freundlich Adsorption Models, *Langmuir*, 28(3), 1790–1803, doi:10.1021/LA2042873, 2012.

335

 Hatch, C. D., Greenaway, A. L., Christie, M. J. and Baltrusaitis, J.: Water adsorption constrained Frenkel–Halsey–Hill adsorption activation theory: Montmorillonite and illite, *Atmos. Environ.*, 87, 26–33, doi:10.1016/J.ATMOSENV.2013.12.040, 2014.


 Herich, H., Tritscher, T., Wiacek, A., Gysel, M., Weingartner, E., Ulrike, L., Urs, B. and J., C. D.: Water uptake of clay and desert dust aerosol particles at sub- and supersaturated water vapor conditions, *Phys. Chem. Chem. Phys.*, 11(36), 7804–7809, doi:10.1039/B901585J, 2009.

340

Hoppel, W. A., Twomey, S. and Wojciechowski, T. A.: A segmented thermal diffusion chamber for continuous measurements of CN, *J. Aerosol Sci.*, 10(4), 369–373, doi:10.1016/0021-8502(79)90031-4, 1979.


Karydis, V. A., Tsimpidi, A. P., Bacer, S., Pozzer, A., Nenes, A. and Lelieveld, J.: Global impact of mineral dust on cloud droplet number concentration, *Atmos. Chem. Phys.*, 17(9), 5601–5621, doi:10.5194/ACP-17-5601-2017, 2017.

345

 Koehler, K. A., Demott, P. J., Kreidenweis, S. M., Popovicheva, O. B., Petters, M. D., Carrico, C. M., Kireeva, E. D., Khokhlova, T. D. and Shonija, N. K.: Cloud condensation nuclei and ice nucleation activity of hydrophobic and hydrophilic soot particles, *Phys. Chem. Chem. Phys.*, 11(36), 7906–7920, doi:10.1039/B905334B, 2009.


Köhler, H.: The nucleus in and the growth of hygroscopic droplets, *Trans. Faraday Soc.*, 32(0), 1152–1161, doi:10.1039/TF9363201152, 1936.

350

 Kumar, P., Nenes, A. and Sokolik, I. N.: Importance of adsorption for CCN activity and hygroscopic properties of mineral dust aerosol, *Geophys. Res. Lett.*, 36(24), L24804, doi:10.1029/2009GL040827, 2009.


Lintis, L., Ouf, F. X., Parent, P., Ferry, D., Laffon, C. and Vallières, C.: Quantification and prediction of water uptake by soot deposited on ventilation filters during fire events, *J. Hazard. Mater.*, 403, 123916, doi:10.1016/J.JHAZMAT.2020.123916, 2021.

355

 Malek, K. A., Gohil, K., Al-Abadleh, H. A. and Asa-Awuku, A. A.: Hygroscopicity of polycatechol and polyguaiacol secondary organic aerosol in sub- and supersaturated water vapor environments, *Environ. Sci. Atmos.*, 2(1), 24–33, doi:10.1039/D1EA00063B, 2022.

Mao, C. N., Malek, K. A. and Asa-Awuku, A.: Hygroscopicity and the water-polymer interaction parameter of nano-sized biodegradable hydrophilic substances, *Aerosol Sci. Technol.*, 55(10), 1115–1124, doi:10.1080/02786826.2021.1931012, 2021.

360

Miles, R. E. H., Rudić, S., Orr-Ewing, A. J. and Reid, J. P.: Sources of Error and Uncertainty in the Use of Cavity Ring Down Spectroscopy to Measure Aerosol Optical Properties, *Aerosol Sci. Technol.*, 45(11), 1360–1375, doi:10.1080/02786826.2011.596170, 2011. 

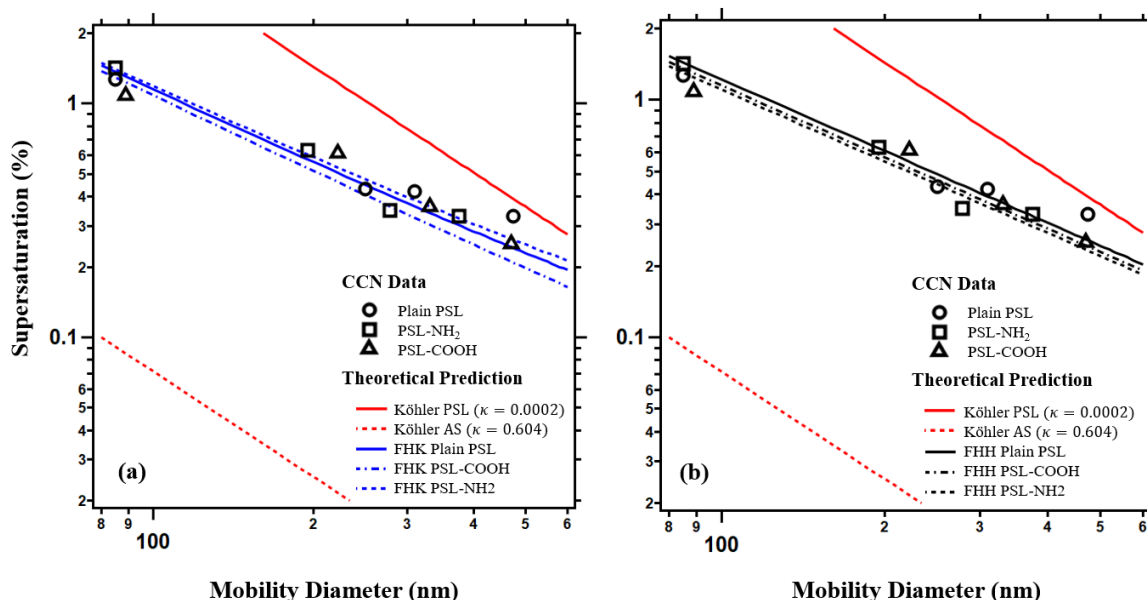
- Moore, R. H., Nenes, A. and Medina, J.: Scanning Mobility CCN Analysis—A Method for Fast Measurements of Size-Resolved CCN Distributions and Activation Kinetics, *Aerosol Sci. Technol.*, 44(10), 861–871, doi:10.1080/02786826.2010.498715, 2010.
- Navea, J. G., Richmond, E., Stortini, T. and Greenspan, J.: Water Adsorption Isotherms on Fly Ash from Several Sources, *Langmuir*, 33(39), 10161–10171, doi:10.1021/ACS.LANGMUIR.7B02028/SUPPL_FILE/LA7B02028_SI_001.PDF, 2017.
- 365 Ottewill, R. H. and Vincent, B.: Colloid and surface chemistry of polymer latices. Part 1.—Adsorption and wetting behaviour of n-alkanols, *J. Chem. Soc. Faraday Trans. 1 Phys. Chem. Condens. Phases*, 68(0), 1533–1543, doi:10.1039/F19726801533, 1972.
- Pajunoja, A., Lambe, A. T., Hakala, J., Rastak, N., Cummings, M. J., Brogan, J. F., Hao, L., Paramonov, M., Hong, J., Prisle, N. L., Malila, J., Romakkaniemi, S., Lehtinen, K. E. J., Laaksonen, A., Kulmala, M., Massoli, P., Onasch, T. B., Donahue, N. M., Riipinen, I., Davidovits, P., Worsnop, D. R., Petäjä, T. and Virtanen, A.: Adsorptive uptake of water by semisolid secondary organic aerosols, *Geophys. Res. Lett.*, 42(8), 3063–3068, doi:10.1002/2015GL063142, 2015.
- 370 Peng, C., Razafindrambina, P. N., Malek, K. A., Chen, L., Wang, W., Huang, R. J., Zhang, Y., Ding, X., Ge, M., Wang, X., Asa-Awuku, A. A. and Tang, M.: Interactions of organosulfates with water vapor under sub- and supersaturated conditions, *Atmos. Chem. Phys.*, 21(9), 7135–7148, doi:10.5194/ACP-21-7135-2021, 2021.
- Peng, C., Malek, K. A., Rastogi, D., Zhang, Y., Wang, W., Ding, X., Asa-Awuku, A. A., Wang, X. and Tang, M.: Hygroscopicity and cloud condensation nucleation activities of hydroxyalkylsulfonates, *Sci. Total Environ.*, 830, 154767, doi:10.1016/J.SCITOTENV.2022.154767, 2022.
- 375 Pethrick, R.: *Polymer physics*. Edited by Michael Rubinstein and Ralph H Colby Oxford University Press, Oxford, 2003. ISBN 019852059X. pp 440, Wiley., 2004.
- Petters, M. D. and Kreidenweis, S. M.: A single parameter representation of hygroscopic growth and cloud condensation nucleus activity, *Atmos. Chem. Phys.*, 7(8), 1961–1971, doi:10.5194/acp-7-1961-2007, 2007.
- 380 Petters, M. D. and Kreidenweis, S. M.: A single parameter representation of hygroscopic growth and cloud condensation nucleus activity - Part 2: Including solubility, *Atmos. Chem. Phys.*, 8(20), 6273–6279, doi:10.5194/ACP-8-6273-2008, 2008.
- Petters, M. D., Kreidenweis, S. M., Snider, J. R., Koehler, K. A., Wang, Q., Prenni, A. J. and Demott, P. J.: Cloud droplet activation of polymerized organic aerosol, *Tellus B Chem. Phys. Meteorol.*, 58(3), 196–205, doi:10.1111/j.1600-0889.2006.00181.x, 2006.
- 385 Petters, M. D., Kreidenweis, S. M., Prenni, A. J., Sullivan, R. C., Carrico, C. M., Koehler, K. A. and Ziemann, P. J.: Role of molecular size in cloud droplet activation, *Geophys. Res. Lett.*, 36(22), L22801, doi:10.1029/2009GL040131, 2009.
- Pettersson, A., Lovejoy, E. R., Brock, C. A., Brown, S. S. and Ravishankara, A. R.: Measurement of aerosol optical extinction at 532 nm with pulsed cavity ring down spectroscopy, *J. Aerosol Sci.*, 35(8), 995–1011, doi:10.1016/j.jaerosci.2004.02.008, 2004.
- 390 Reitz, P., Spindler, C., Mentel, T. F., Poulain, L., Wex, H., Mildenerger, K., Niedermeier, D., Hartmann, S., Claus, T., Stratmann, F., Sullivan, R. C., Demott, P. J., Petters, M. D., Sierau, B. and Schneider, J.: Surface modification of mineral dust particles by sulphuric acid processing: Implications for ice nucleation abilities, *Atmos. Chem. Phys.*, 11(15), 7839–7858, doi:10.5194/ACP-11-7839-2011, 2011.
- Roberts, G. C. and Nenes, A.: A Continuous-Flow Streamwise Thermal-Gradient CCN Chamber for Atmospheric Measurements, *Aerosol Sci. Technol.*, 39(3), 206–221, doi:10.1080/027868290913988, 2005.
- 395 Rose, D., Gunthe, S. S., Mikhailov, E., Frank, G. P., Dusek, U., Andreae, M. O. and Pöschl, U.: Calibration and measurement uncertainties of a continuous-flow cloud condensation nuclei counter (DMT-CCNC): CCN activation of ammonium sulfate and sodium chloride aerosol particles in theory and experiment, *Atmos. Chem. Phys.*, 8(5), 1153–1179, doi:10.5194/ACP-8-1153-2008, 2008.
- 400 Singh, S., Fiddler, M. N., Smith, D. and Bililign, S.: Error analysis and uncertainty in the determination of aerosol optical properties using cavity ring-down spectroscopy, integrating nephelometry, and the extinction-minus-scattering method, *Aerosol Sci. Technol.*, 48(12), 1345–1359, doi:10.1080/02786826.2014.984062, 2014.
- Sorjamaa, R. and Laaksonen, A.: The effect of H₂O adsorption on cloud drop activation of insoluble particles: a theoretical framework. [online] Available from: www.atmos-chem-phys.net/7/6175/2007/ (Accessed 17 January 2021a), 2007.
- 405 Sorjamaa, R. and Laaksonen, A.: The effect of H₂O adsorption on cloud drop activation of insoluble particles: A theoretical framework, *Atmos. Chem. Phys.*, 7(24), 6175–6180, doi:10.5194/ACP-7-6175-2007, 2007b.

Sullivan, R. C., K Moore, M. J., Petters, M. D., Kreidenweis, S. M., Roberts, G. C. and Prather, K. A.: Atmospheric Chemistry and Physics Effect of chemical mixing state on the hygroscopicity and cloud nucleation properties of calcium mineral dust particles. [online] Available from: www.atmos-chem-phys.net/9/3303/2009/ (Accessed 20 March 2020), 2009.

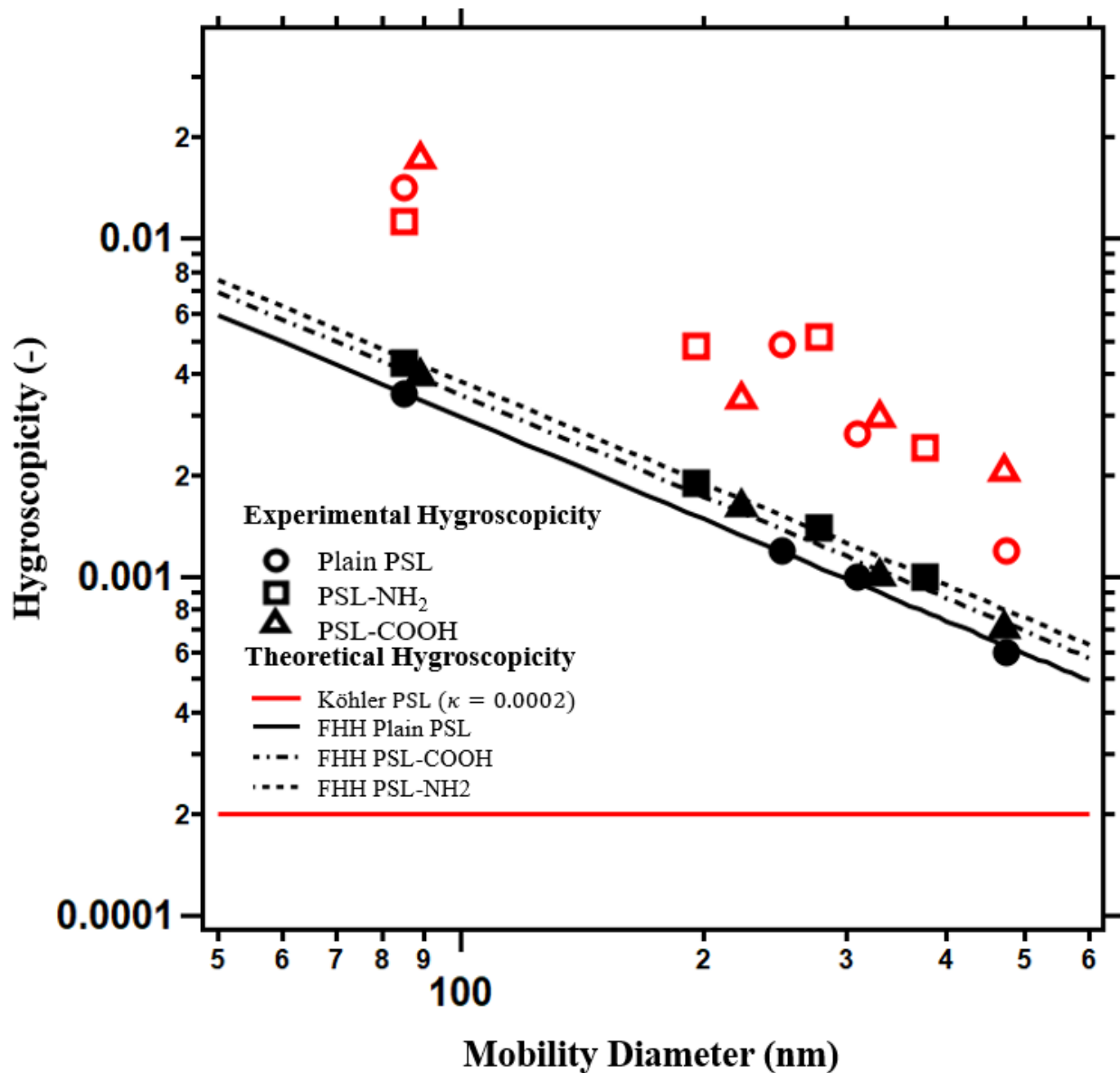
410 Sullivan, R. C., Petters, M. D., Demott, P. J., Kreidenweis, S. M., Wex, H., Niedermeier, D., Hartmann, S., Clauss, T., Stratmann, F., Reitz, P., Schneider, J. and Sierau, B.: Irreversible loss of ice nucleation active sites in mineral dust particles caused by sulphuric acid condensation, *Atmos. Chem. Phys.*, 10(23), 11471–11487, doi:10.5194/ACP-10-11471-2010, 2010.

Tang, M., Cziczo, D. J. and Grassian, V. H.: Interactions of Water with Mineral Dust Aerosol: Water Adsorption, Hygroscopicity, Cloud Condensation, and Ice Nucleation, *Chem. Rev.*, 116(7), 4205–4259, doi:10.1021/ACS.CHEMREV.5B00529, 2016.

415 Wang, S. C. and Flagan, R. C.: Scanning electrical mobility spectrometer, *Aerosol Sci. Technol.*, 13(2), 230–240, doi:10.1080/02786829008959441, 1990.



420 Figure 1: The s_c - D_0 data for different types of PSL. The dashed red line is the tradition Köhler prediction for ammonium sulfate ($\kappa = 0.604$). All types of PSL particles are more hygroscopic than the intrinsic hygroscopicity ($\kappa_{int} = 0.0002$, red solid line). (a) Blue lines show the prediction from FHK. (b) Black lines show the prediction from FHH-AT model, with $B_{FHH} = 1$.



425

Figure 2: The single hygroscopicity parameter predicted from FHH-AT and traditional Köhler theory. Köhler theory from intrinsic properties (solid red line) predicts a constant hygroscopicity across particle sizes and hygroscopicity derived from experimental data (open symbols) shows size dependence. Hygroscopicity derived from FHH-AT model from theory (solid black lines) and from experimental data (black symbols) are size dependent and agree well. Hygroscopicity derived from FHH-AT model is also sensitive to surface chemistry functional.

430